Journal of Alloys and Compounds 509 (2011) L56–L58

Contents lists available at ScienceDirect

Journal of Alloys and Compounds

journal homepage: www.elsevier.com/locate/jallcom

Letter

Influence of B_2O_3 additives on microstructure and electrical properties of $ZnO–Bi_2O_3–Sb_2O_3$-based varistors

Fenghua Liu*, Gaojie Xu, Lei Duan, Yali Li, Yong Li, Ping Cui

Ningbo Institute of Material Technology and Engineering (NIMTE), Chinese Academy of Sciences (CAS), Ningbo 315201, People's Republic of China

ARTICLE INFO

Article history:
Received 18 April 2010
Received in revised form 22 October 2010
Accepted 22 October 2010
Available online 29 October 2010

Keywords:
Ceramics
Varistors
Sintering
Boron oxide
Nonlinear

ABSTRACT

B_2O_3-doped $ZnO–Bi_2O_3–Sb_2O_3$-based varistors were fabricated by conventional ceramic technique. The microstructure and electrical properties were investigated by SEM, XRD and electrical measurements. With the addition of B_2O_3, the liquid-assisted sintering based on Bi_2O_3 was improved, and the $Bi_2O_3–B_2O_3$ glass and $Zn_3(BO_3)_2$ phase were formed on the grain boundaries. The doping of B_2O_3 markedly improved the varistor performance of the $ZnO–Bi_2O_3–Sb_2O_3$-based varistors. The nonlinear coefficient of the sample with 3.5 mol% B_2O_3 sintered at 1100 °C reached 56 and the leakage current was only 0.3 μA.

1. Introduction

ZnO varistors are ceramic semiconductor devices, which are obtained by sintering ZnO powder with small amounts of other metal oxides [1,2]. ZnO varistors exhibit highly nonlinear current–voltage ($I–V$) characteristics, similar to that of "back-to-back" zener diodes but with much greater current- and energy-handling capabilities. These characteristics make ZnO varistors very attractive as arresters or surge absorbers against electric power system overvoltage or electronic circuit surges [3,4].

The nonlinear current–voltage ($I–V$) characteristics of ZnO varistors strongly depend on the presence of minor additives. The additives can be classified into two general categories. One is the main additives, termed 'varistors formers', without which varistor behavior cannot be obtained, such as Bi_2O_3, Pr_6O_{11}, V_2O_5 and lead zinc borosilicate glass [5–10]; the other is the assistant additives, which are metal oxides, including Co, Mn, Cr, Al, Ni, Sb and Ti oxides [4,11]. In present, the majority of commercially available varistors are based on $ZnO–Bi_2O_3$ systems where Bi_2O_3 plays an essential role in liquid sintering and the forming of nonlinear behavior [12–15]. Other dopants, such as Sb_2O_3, Cr_2O_3, CoO, NiO and MnO_2, are added as assistant additives to increase the nonlinear coefficient (α) value and the resistance to degradation [16–18].

The nonlinear effect of ZnO varistors is controlled by grain boundary barriers. Therefore, the number of active or effective barriers in the ceramics is an important parameter for the nonlinear properties. The number of active barriers depends on the distribution of dopants and the sintering process. B_2O_3 is a low melting point oxide, which is often used as an additive of liquid sintering in the ceramic processing. Previous studies had shown that B_2O_3 plays an important role in ZnO–PbO-based system [19]. However, little study has been devoted to the influence of B_2O_3 additives on the $ZnO–Bi_2O_3–Sb_2O_3$ based varistors. In this paper, we carried out a detailed study of $ZnO–Bi_2O_3–Sb_2O_3$ based varistors doped with 0–5.5 mol% B_2O_3. The results indicated that the doping of B_2O_3 effectively improved the electrical properties.

2. Experimental procedures

The samples were fabricated using a conventional ceramic process [17,18], with a nominal composition of $(97-x)$ mol% ZnO + 1.0 mol% Bi_2O_3 + 1.0 mol% Sb_2O_3 + 0.2 mol% Co_2O_3 + 0.2 mol% MnO_2 + 0.3 mol% Cr_2O_3 + 0.3 mol% NiO + x mol% B_2O_3 (x = 0.0, 1.5, 2.5, 3.5, 4.5, 5.5). The powder mixtures were ball-milled in a polyethylene bottle with ZrO_2 balls for 24 h in deionized water. After dried and granulated, the powder was pressed into discs of 15 mm in diameter and 1.2 mm in thickness at a pressure of 80 MPa. The discs were sintered between 1050 °C and 1200 °C in air for 2 h, with heating rate of 300 °C/h and cooling naturally. The final samples were pasted with silver on both faces and then heated at 300 °C for 10 min to form ohmic contacts.

The phase composition of the samples was analyzed by a Rigaku D/Max-A diffractometer with Cu Kα radiation. The microstructure was examined using a Hitachi S4800 field emission scanning election microscope (FESEM). The average grain size (d) was determined by the linear intercept method. The $I–V$ characteristics of samples were measured using Keithley 237. The breakdown voltage ($V_{1\,mA}$) was measured at a current density of 1.0 mA/cm^2, and the leakage current (I_L) was measured at 0.80 $V_{1\,mA}$. The nonlinear coefficient (α) was determined from $\alpha = \log(I_2/I_1)/\log(V_2/V_1)$, where I_1 = 0.1 mA/cm^2, I_2 = 1.0 mA/cm^2, and V_1 and V_2 are the electric fields corresponding to I_1 and I_2, respectively.

* Corresponding author.
E-mail address: lfh@nimte.ac.cn (F. Liu).

0925-8388/$ – see front matter © 2010 Elsevier B.V. All rights reserved.
doi:10.1016/j.jallcom.2010.10.074

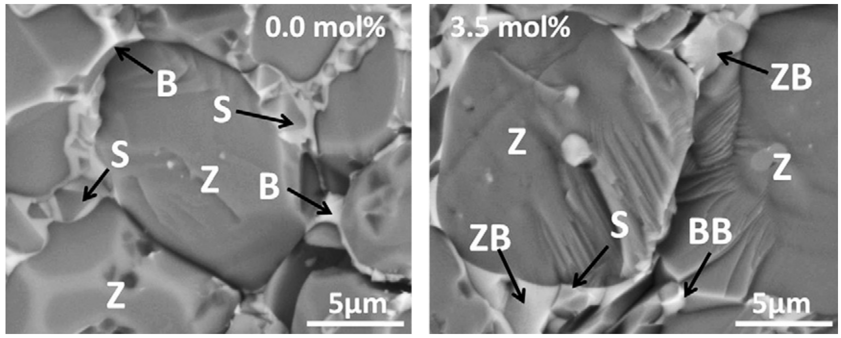

Fig. 1. The SEM micrographs of the specimens with 0 mol% and 3.5 mol% B_2O_3 contents (Z: ZnO, S: spinel phase, B: Bi_2O_3 phase, ZB: $Zn_3(BO_3)_2$ phase, BB: Bi_2O_3–B_2O_3 glass).

3. Results and discussion

Fig. 1 shows the SEM micrographs of the specimens sintered at 1100 °C for 2 h with 0 mol% and 3.5 mol% B_2O_3. One can see that the microstructure of the specimens is consisted of ZnO grain (bulk phase) and intergranular layer (second phase). The XRD patterns of the specimens sintered at 1100 °C for 2 h with different amounts of B_2O_3 are displayed in Fig. 2. The XRD patterns show that the second phase located at the boundaries was consisted of $Zn_{2.33}Sb_{0.67}O_4$ spinel phase and Bi_2O_3 phase without the addition of B_2O_3. As the addition of B_2O_3, the Bi_2O_3 phase vanished and a new phase of $Zn_3(BO_3)_2$ was formed. This change of the second phase is different from the previous reported B_2O_3-contained ZnO varistors [20,21]. The disappearance of Bi_2O_3 phase indicated that the B_2O_3 reacted with Bi_2O_3 to form Bi_2O_3–B_2O_3 glass [22]. And, the formation of $Zn_3(BO_3)_2$ expressed that the B_2O_3 also reacted with ZnO grain through reaction (1):

$$3ZnO + B_2O_3 = Zn_3(BO_3)_2 \quad (1)$$

The average ZnO grain size (d) and the density (ρ) of the specimens sintered at 1100 °C for 2 h with different amounts of B_2O_3 are displayed in Fig. 3. The results show that the average ZnO grain size (d) increased with the increase of B_2O_3 content, then decreased while the added amount was beyond 3.5 mol%. It is well known that the liquid-assisted sintering often plays an important role in the growth of grains. Previous studies had shown that the growth of ZnO grains depends on the liquid-assisted sintering based on Bi_2O_3 [12,14]. For B_2O_3 added ZnO–Bi_2O_3–Sb_2O_3-based ceramics, the low melting point B_2O_3 is doped together with Bi_2O_3 that causes the liquid-phase sintering and growth of ZnO grains start at a lower temperature and further accelerates the growth of ZnO grains. However, B_2O_3 also reacts with ZnO grain through reaction (1), which leads to the formation of $Zn_3(BO_3)_2$ on the grain boundaries. It may inhibit grain growth by pinning the movement of the grain boundaries. Therefore, the ZnO grain size (d) does not monotonically increase with the increase of B_2O_3 content. Fig. 3 also shows that with the increase of B_2O_3 content, the density (ρ) of the specimens increased first and then decreased.

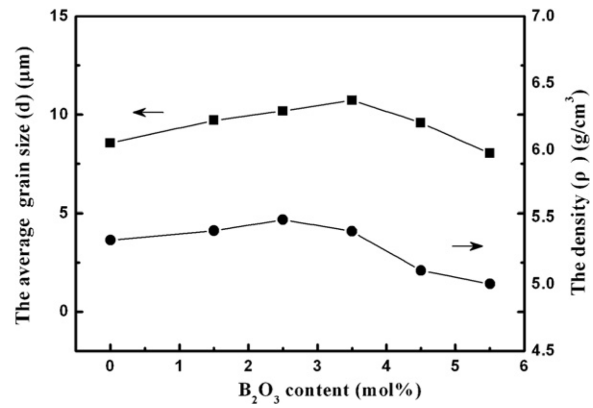

Fig. 3. The average ZnO grain size (d) and the density (ρ) of the specimens with different amounts of B_2O_3 sintered at 1100 °C for 2 h.

The breakdown field $V_{1\,mA}$ as a function of B_2O_3 content is presented in Fig. 4. The sintering temperature of the specimens was 1100 °C. Fig. 4 indicates the breakdown field $V_{1\,mA}$ increased with the increase of B_2O_3 content, then decreased while the added amount was beyond 3.5 mol%. This can be explained by the change of the average grain size as shown in Fig. 3.

The nonlinear coefficient (α) and leakage current density (I_L) as a function of B_2O_3 content are presented in Fig. 5. The results show that the doping of B_2O_3 had an obvious effect on the nonlin-

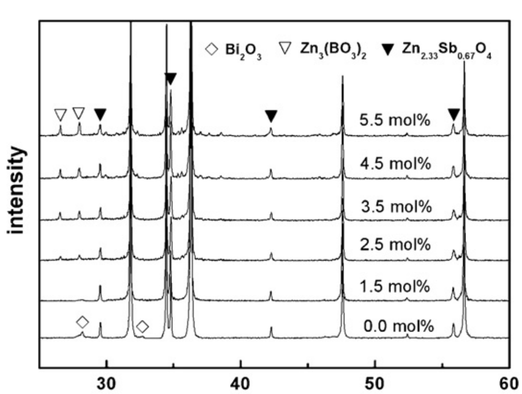

Fig. 2. XRD profiles of the specimens sintered at 1100 °C for 2 h with different amounts of B_2O_3 (0.0 mol%, 1.5 mol%, 2.5 mol%, 3.5 mol%, 4.5 mol%, 5.5 mol%).

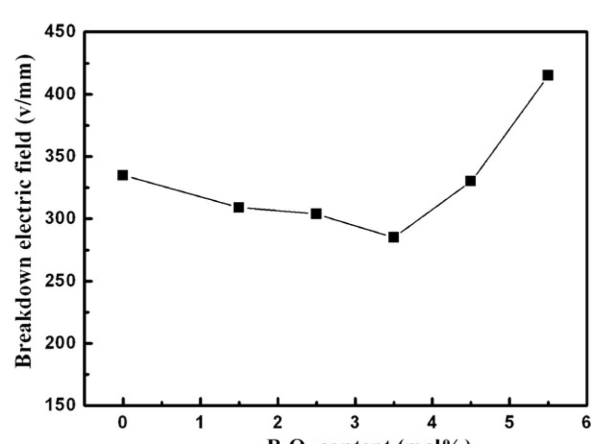

Fig. 4. The breakdown field of B_2O_3-doped ZnO varistors sintered at 1100 °C for 2 h.

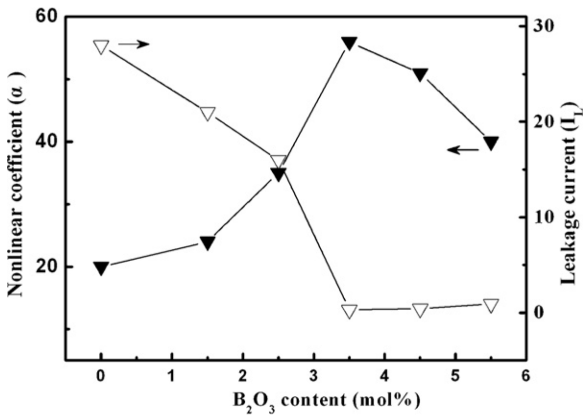

Fig. 5. The nonlinear coefficient (α) and leakage current density (I_L) of B_2O_3-doped ZnO varistors sintered at 1100 °C for 2 h.

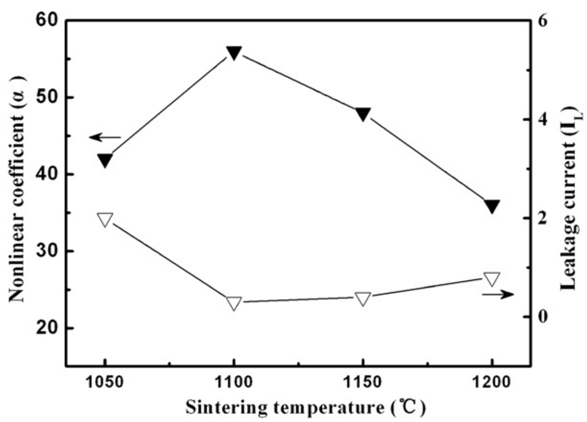

Fig. 6. The nonlinear coefficient (α) and leakage current density (I_L) of the samples with B_2O_3 content of 3.5 mol% sintered at different temperature.

ear coefficient (α) and leakage current density (I_L) of the samples. With increasing B_2O_3 content, the nonlinear coefficient (α) showed opposite changes to the leakage current. A nonlinear coefficient of 56 was obtained for the sample with B_2O_3 content of 3.5 mol%, and the leakage current was only 0.3 μA.

The improvement of the electrical properties may be attributed to the influence of B_2O_3 on the ZnO grain and intergranular layer. For the B_2O_3 added samples, part of the B^{3+} ions are probably dissolved into the interstitials of ZnO lattice or substituted for Zn [23], which will increase the conductivity of ZnO grain by supplying extra conduction electrons, as can be illustrated as reaction (2):

$$2B_2O_3 \rightarrow 4B_{Zn}^{\cdot} + 3O_2 + 4e^- \quad (2)$$

In addition, the low melting point B_2O_3 can improve the liquid-assisted sintering based on Bi_2O_3. The improved liquid-assisted sintering ensures a more uniform distribution of dopants over the sintered body and, hence, increases the number of the active or effective boundary barriers in the ceramics and improves the nonlinear behavior of the $ZnO–Bi_2O_3–Sb_2O_3$-based ceramics.

However, when the doping level of B_2O_3 is much high, too more liquid-phase would be formed during sintering, which may cause the immoderate growth of ZnO and lead to an inhomogeneous increase of grain sizes. Hence, the nonlinear coefficient (α) decreased and the leakage current density (I_L) increased while the added B_2O_3 content was beyond 3.5 mol%. The influence of different sintering temperature on the nonlinear coefficient (α) and leakage current density (I_L) of the samples with B_2O_3 content of 3.5 mol% is presented in Fig. 6. The sample sintered at 1100 °C exhibited the best performance.

4. Conclusions

The microstructure and the electrical properties of B_2O_3-doped $ZnO–Bi_2O_3–Sb_2O_3$-based varistors were investigated. With the addition of B_2O_3, the liquid-assisted sintering based on Bi_2O_3 was improved, and the $Bi_2O_3–B_2O_3$ glass and $Zn_3(BO_3)_2$ phase were formed on the grain boundaries. The *I–V* characteristics of the samples indicated that the doping of B_2O_3 can effectively enhance the varistor performance. The nonlinear coefficient of the varistors with B_2O_3 content of 3.5 mol% sintered at 1100 °C reached 56 and the leakage current was only 0.3 μA.

Acknowledgements

This work was supported by the Key Technologies R&D Program of Ningbo (No. 2008B10049), Zhejiang Provincial Natural Science Foundation of China (Grant nos. D4080489 and Y4090044), Ningbo Natural Science Foundation (2009A610031 and 2010A610170). We also express our gratitude to the aided program for Science and Technology Innovative Research Team of Zhejiang Province and Ningbo Municipality (2009B21005).

References

[1] M. Matsuoka, Jpn. J. Appl. Phys. 10 (1971) 736–746.
[2] G.G. Zhao, R.P. Joshi, H.P. Hjalmarson, J. Am. Ceram. Soc. 91 (2008) 1188–1193.
[3] K. Sato, Y. Takada, T. Takemura, M. Ototake, J. Appl. Phys. 53 (1982) 8819–8826.
[4] T.K. Gupta, J. Am. Ceram. Soc. 73 (1990) 1817–1840.
[5] J.V. Bellini, M.R. Morelli, R.H.G.A. Kiminami, Mater. Lett. 62 (2008) 335–337.
[6] Z.J. Peng, X.F. Fu, Y.X. Zang, Z.Q. Fu, C.B. Wang, L.H. Qi, H.Z. Miao, J. Alloys Compd. 508 (2010) 494–499.
[7] H. Feng, Z.J. Peng, X.I. Fu, Z.Q. Fu, C.B. Wang, L.H. Qi, H.Z. Miao, J. Alloys Compd. 497 (2010) 304–307.
[8] H.H. Hng, L. Halim, Mater. Lett. 57 (2003) 1411–1416.
[9] C.W. Nahm, J. Alloys Compd. 505 (2010) 657–660.
[10] S. Bernik, N. Daneu, A. Recnik, J. Eur. Ceram. Soc. 24 (2004) 3703–3708.
[11] C.W. Nahm, J. Alloys Compd. 490 (2010) L52–L54.
[12] D. Dey, R.C. Bradt, J. Am. Cream. Soc. 75 (1992) 2529–2534.
[13] Y.W. Lao, S.T. Kuo, W.H. Tuan, J. Mater. Sci. Mater. Electron. 20 (2009) 234–241.
[14] L. Cong, X. Zheng, P. Hu, S. Dan-Feng, J. Am. Cream. Soc. 90 (2007) 2791–2794.
[15] K.Y. Yuan, G.R. Li, L.Y. Zheng, L.H. Cheng, L. Meng, Z. Yao, Q.R. Yin, J. Alloys Compd. 503 (2010) 507–513.
[16] S. Bernik, J. Bernard, N. Daneu, A. Recnik, J. Am. Cream. Soc. 90 (2007) 3239–3247.
[17] Y.C. Chen, C.Y. Shen, H.Z. Chen, Y.F. Wei, L. Wu, Jpn. J. Appl. Phys. 30 (1991) 84–90.
[18] S.A. Pianaro, E.C. Pereira, L.O.S. Bulhoes, E. Longo, J.A. Varela, J. Mater. Sci. 30 (1995) 133–141.
[19] W. Jun, C.S. Xie, J.H. Hu, D.W. Zeng, A.H. Wang, J. Eur. Ceram. Soc. 24 (2004) 3635–3641.
[20] J.L. Huang, K.B. Li, J. Mater. Res. 9 (1994) 1526–1532.
[21] F.H. Liu, G.J. Xu, L. Duan, Y.L. Li, P. Cui, Key Eng. Mater. 368–371 (2008) 497–499.
[22] Y. Cheng, H.N. Xiao, W.M. Guo, W.M. Guo, Thermochim. Acta 444 (2006) 173–178.
[23] T.K. Gupta, W.G. Carlson, J. Mater. Sci. 20 (1985) 3487–3500.